

000 001 FEDQAPER: QUERY ATTENTION POOLING FOR DI- 002 MENSION ALIGNMENT IN FEDERATED NON-IID TIME- 003 SERIES FORECASTING WITH PERSONALIZED HEADS 004 005

006 **Anonymous authors**
007 Paper under double-blind review
008
009
010
011

ABSTRACT

013 Federated learning (FL) has shown great promise for time-series forecasting, yet
014 a key challenge in real-world applications is feature heterogeneity. Unlike prior
015 work that assumes uniform feature spaces, we construct a more realistic feature-
016 level non-independent and identically distributed (non-IID) scenario by allocating
017 subsets of features to each client. The number of features varies from 1 up to
018 a defined maximum. We introduce FedQAPER, a novel FL framework that com-
019 bines Query Attention Pooling (QAP) with FedPer algorithm that uses personal-
020 ized heads for each client to capture local patterns. QAP projects heterogeneous
021 client feature dimensions into a unified representational space, enabling collabo-
022 rative backbone training across diverse feature configurations. FedPer transforms
023 these aligned representations back to each client’s original feature dimension
024 through personalized heads, achieving both global knowledge integration and lo-
025 cal specialization. FedQAPER works for various backbone architectures, including
026 both artificial neural network (ANN) models and spiking neural network (SNN)
027 models. Experiments on multivariate time-series benchmarks demonstrate that
028 FedQAPER effectively handles feature heterogeneity and consistently improves
029 forecasting performance across different backbone models.

030 1 INTRODUCTION 031

032 Time-series forecasting is fundamental to modern data-driven systems, enabling proactive decision-
033 making in diverse fields such as renewable energy management (Gaboitaoelwe et al. (2023)) and
034 smart grid (Aslam et al. (2021)). For these tasks, deep learning models have demonstrated strong
035 performance. Artificial Neural Networks (ANNs), particularly recurrent and attention-based archi-
036 tectures, have emerged as a dominant paradigm due to their unparalleled ability to capture intricate
037 temporal dependencies and long-range patterns within data (Zhou et al. (2022); Wang et al.
038 (2024c); Nie et al. (2023)). Meanwhile, Spiking Neural Networks (SNNs) offer a distinct, com-
039 pelling advantage in energy efficiency and suitability for resource-constrained edge devices (Feng
040 et al. (2025); Hu et al. (2025)). By encoding temporal patterns through discrete spike events, SNNs
041 can dramatically reduce energy consumption and computational overhead compared to conventional
042 ANNs (Yu et al. (2024a); Skatchkovsky et al. (2019); Wen et al. (2023)). Recent advances in neuro-
043 morphic computing further demonstrate that SNN-based federated learning can maintain competi-
044 tive forecasting accuracy while achieving significant improvements in energy and communication
045 efficiency (Li et al. (2025); Venkatesha et al. (2021)). Given the complementary strengths of both
046 ANNs and SNNs, both are excellent candidates for various time-series forecasting tasks.

047 Traditional time series forecasting relies on centralized training paradigms that aggregate all data
048 onto a single server (Xu et al. (2024); donghao & wang xue (2024)). However, this approach raises
049 significant privacy concerns and creates substantial communication overhead, particularly problem-
050 atic in distributed environments (Abdel-Sater & Hamza (2024)). To address these limitations, fed-
051 erated learning (FL) such as FedAvg (McMahan et al. (2023)) has emerged as a promising solution
052 that enables collaborative model training across decentralized edge devices without sharing raw data,
053 thus preserving privacy and reducing communication costs (Zhao et al. (2018)). Yet, they largely ig-
054 nore a critical challenge in real-world applications: feature-level non-independent and identically
055 distributed (non-IID), where clients possess different sets of input features. Existing FL frame-
056

054 works typically require a uniform feature space, making them ill-suited for such scenarios(Li et al.
 055 (2020);Ghosh et al. (2021);Karimireddy et al. (2021)) . This limitation is particularly pronounced in
 056 real-world deployments such as heterogeneous IoT devices in smart grids or transportation systems,
 057 where devices may have different sensor configurations and data collection capabilities.

058 To overcome this critical limitation, we introduce FedQAPer, a novel FL framework specifically
 059 designed to handle feature-level non-IID data in time-series forecasting. Our method enables clients
 060 with diverse feature configurations to collaboratively train a global model while maintaining both
 061 privacy and efficiency. Our key contributions are as follows:
 062

- 063 • **Realistic feature-level non-IID formulation:** Unlike prior work that assumes identical
 064 feature spaces, we explicitly construct a more realistic FL setting where each client has a
 065 different number and type of features. This better reflects real-world deployments, such as
 066 heterogeneous IoT devices in smart grids or transportation systems.
- 067 • **Query Attention Pooling (QAP):** We propose QAP to align heterogeneous client features
 068 into a unified latent space. This alignment enables consistent backbone training across
 069 clients despite their varying feature dimensions.
- 070 • **Personalized Federated Learning via FedPer:** We incorporate the FedPer algo-
 071 rithm(Arivazhagan et al. (2020)), equipping each client with lightweight personalized
 072 heads. These heads map the QAP-aligned representations back to the client’s original fea-
 073 ture space, achieving both global knowledge sharing and local specialization.
- 074 • **Backbone-Agnostic Design:** FedQAPer is compatible with a wide range of backbone
 075 architectures, including both ANN and SNN models, ensuring flexibility and broad appli-
 076 cability.

077 2 RELATED WORKS

078 2.1 FEATURE DISTRIBUTION IN FEDERATED TIME-SERIES FORECASTING

079 FL has recently been explored in time-series forecasting, where distributed clients such as sensors,
 080 base stations, or smart meters collaboratively learn forecasting models without centralizing raw
 081 data (Fekri et al. (2022)). A key challenge in this domain is the inherent non-IID nature of local
 082 data. Prior studies typically assume that clients share identical feature spaces, while heterogeneity
 083 primarily arises from different in data distribution, sample sizes, or temporal dynamics.

084 For instance, Fed-TREND (Yuan et al. (2024)) addresses data heterogeneity by treating each fea-
 085 ture (or a subset of features) from a single dataset as a distinct client, which then collectively trains
 086 various forecasting models. Some approaches may partition a single dataset to match the number
 087 of clients, ensuring that each client holds the same set of features(Maher et al. (2025)). Other stud-
 088 ies treat an entire dataset as a single client for cross-domain feature heterogeneity. For example,
 089 TIME-FFM(Liu et al. (2024a)) uses general time-series datasets like ETT(Zhou et al. (2021) and
 090 Electricity(Lai et al. (2018)) as individual clients, while HSTFL(Cai & Liu (2024)) holds a unique
 091 type of time series data, with the data types varying among different clients. It is also possible to
 092 configure clients with multiple datasets from the same domain, rather than from different domains.
 093 FedWindT(Arooj (2024)) considers the dataset from each wind power plant, which contains data
 094 on wind speed, temperature, and output, as a separate client to predict the power generation of that
 095 plant.These methods implement non-IID conditions by creating differences in the feature charac-
 096 teristics of clients. FedAtt (Thwal et al. (2023)) predicts the next day’s closing price returns for
 097 each of the 45 publicly traded companies using their stock-related data. Non-IID data can also be
 098 achieved by varying the time frequency of data across clients, as seen in works like MVFL(Yang
 099 et al. (2025)) and FedForecast(Liu et al. (2023)). However, there is limited research on distributing
 100 a different number of features from a single dataset to clients.

101 2.2 SPIKING NEURAL NETWORK IN FEDERATED LEARNING

102 The integration of SNNs with FL offers a promising direction for streamlined, privacy-preserving AI
 103 on resource-constrained edge devices. SNNs’ event-driven, sparse communication inherently pro-
 104 vides high computational performance and low power consumption. Capitalizing on these advan-
 105 tages, FedLEC (Yu et al. (2025)) presented an effective FL algorithm that utilizes SNNs to mitigate
 106

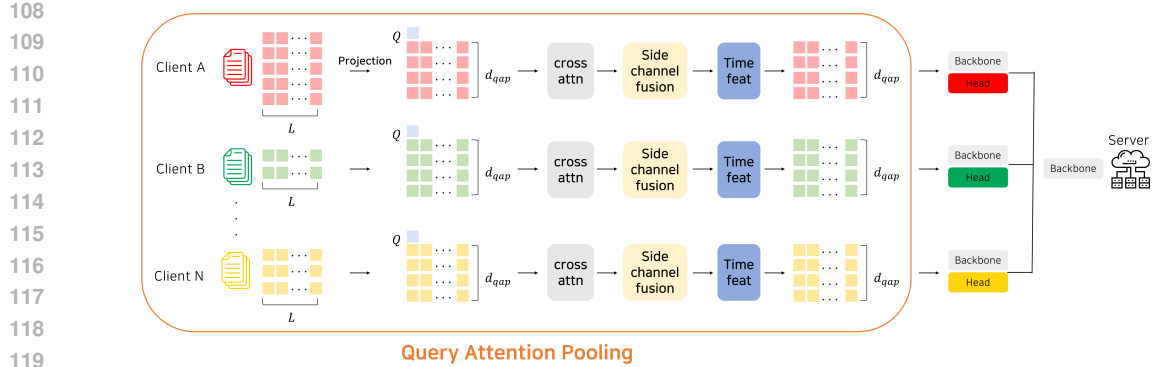


Figure 1: Overview of the proposed FEDQAPER framework.

label skewness and improve convergence in non-IID settings. Xie et al. (2022) demonstrated SNNs' effectiveness in FL for specific application, such as traffic sign recognition in resource-limited Internet of Vehicles scenarios. Beyond homogeneous model architectures, heterogeneous FL combining convolutional and SNNs has also been explored Yu et al. (2024b). These collective efforts highlight SNNs' significant potential for enabling robust and resource-friendly FL deployments, particularly where computational and communication resources are limited. Despite these advancements, the predominant focus of current SNN-FL research largely remains on classification tasks.

3 FEDQAPER

Figure 1 provides an overview of the proposed FedQAPER framework, illustrating the end-to-end pipeline from heterogeneous client inputs through QAP alignment and backbone training to personalized heads for forecasting.

3.1 FEATURE ALLOCATION FOR HETEROGENEOUS CLIENT DATA

To simulate feature-level heterogeneity across clients, we construct each client by randomly assigning it a subset of features from a universal dataset, where each feature corresponds to a variate in the multivariate time series. Specifically, given the number of clients N and a maximum feature count F_{max} , each client is assigned a unique feature subset. The size of this subset is sampled uniformly, ranging from a single feature up to F_{max} features. This design ensures that the dimensionality of the input space varies across clients. For example, some clients may observe only a single variable, while others access a much richer set of features. Feature assignment is performed independently for each client, without coordination or alignment. This random assignment reflects real-world deployments where local devices or sensors monitor distinct and potentially disjoint subsets of variables, depending on hardware constraints or installation context. Once clients are constructed, each client directly feeds its raw features into the federated model.

3.2 QUERY ATTENTION POOLING

In federated time-series forecasting, each client observes a distinct subset of features, leading to heterogeneous input dimensionalities. Let $x^{(i)} \in \mathbb{R}^{B \times L \times F_i}$ denote the input of client i with batch size B , sequence length L , and feature count F_i . Since F_i varies across clients, directly sharing a backbone is infeasible without reconciling dimensional mismatch. We introduce **Query Attention Pooling (QAP)**, a lightweight module that maps arbitrary client features into a unified representational space of dimension d_{qap} . The QAP procedure consists of five steps:

(1) Value projection with slot embedding. Each raw feature value at each time step is projected from scalar to d_{qap} dimensions through a linear transformation, $\text{Linear}(1, d_{qap})$. Each feature channel is then augmented with a learnable client-specific slot embedding $s_j^{(i)} \in \mathbb{R}^{d_{qap}}$ for client i and

162 feature j :

163
$$\mathbf{v}_{t,j} = \text{Linear}(x_{t,j}^{(i)}) + \mathbf{s}_j^{(i)},$$

164 where $x_{t,j}^{(i)}$ is the raw value of feature j at time t for client i .165 **(2) Cross-attention with shared queries.** For each time step independently, the projected feature
166 representations serve as keys and values, while a small set of learnable query vectors $\mathbf{Q} \in \mathbb{R}^{Q \times d_{\text{qap}}}$
167 (typically $Q = 1$) attend to them through multi-head cross-attention with h heads:
168

169
$$\mathbf{z}_t = \text{MultiHeadAttention}(\mathbf{Q}, \{\mathbf{v}_{t,j}\}_{j=1}^{F_i}, \{\mathbf{v}_{t,j}\}_{j=1}^{F_i}).$$

170 **(3) Statistical side-channel fusion.** To ensure robustness when feature counts vary drastically or
171 when attention becomes unstable, QAP incorporates statistical summaries across the feature dimen-
172 sion at each time step:
173

174
$$\mathbf{mean}_t = \frac{1}{F_i} \sum_{j=1}^{F_i} \mathbf{v}_{t,j}, \quad \mathbf{max}_t = \max_{j=1, \dots, F_i} \mathbf{v}_{t,j}.$$

175 These are concatenated with the attention output and fused through a two-layer feedforward net-
176 work:
177

178
$$\mathbf{z}'_t = \text{FFN}([\mathbf{z}_t; \mathbf{mean}_t; \mathbf{max}_t]),$$

179 where $[\cdot; \cdot; \cdot]$ denotes concatenation.
180181 **(4) Query dimension removal.** When using a single query ($Q = 1$), the query dimension is re-
182 moved, yielding the aligned representation
183

184
$$\mathbf{z}_t^{(i)} = \mathbf{z}'_t \in \mathbb{R}^{d_{\text{qap}}}.$$

185 The complete sequence representation becomes $\mathbf{Z}^{(i)} \in \mathbb{R}^{B \times L \times d_{\text{qap}}}$.
186187 **(5) Time feature integration.** To incorporate temporal context while maintaining dimensional con-
188 sistency, time features $\mathbf{t}^{(i)} \in \mathbb{R}^{B \times L \times t_{\text{dim}}}$ are linearly projected into the same latent space:
189

190
$$\mathbf{t}_{\text{emb}}^{(i)} = \text{Linear}(\mathbf{t}^{(i)}) \in \mathbb{R}^{B \times L \times d_{\text{qap}}}.$$

191 The QAP-processed features $\mathbf{Z}^{(i)}$ and time embeddings $\mathbf{t}_{\text{emb}}^{(i)}$ are then concatenated and projected to
192 maintain the target dimensionality:
193

194
$$\mathbf{Z}_{\text{final}}^{(i)} = \text{Linear}([\mathbf{Z}^{(i)}; \mathbf{t}_{\text{emb}}^{(i)}]) \in \mathbb{R}^{B \times L \times d_{\text{qap}}}.$$

195 To summarize, we apply Layer Normalization to $\mathbf{v}_{t,j}$ (the value projection with slot embedding)
196 before attention, and dropout to the attention output. Multi-head attention uses h heads with dot-
197 product scaling. The side-channel feed-forward network (FFN) maps the concatenation
198

199
$$[\mathbf{z}_t; \mathbf{mean}_t; \mathbf{max}_t] \in \mathbb{R}^{3d_{\text{qap}}}$$

200 back to $\mathbb{R}^{d_{\text{qap}}}$. After concatenating time embeddings, a linear layer maps from $\mathbb{R}^{2d_{\text{qap}}}$ back to $\mathbb{R}^{d_{\text{qap}}}$,
201 ensuring that the backbone always receives inputs in
202

203
$$\mathbb{R}^{B \times L \times d_{\text{qap}}}.$$

204 This design ensures that both raw feature information and temporal context are jointly encoded in
205 the unified d_{qap} -dimensional space, enabling seamless integration with any backbone architecture.
206 The complete QAP procedure is also summarized in Algorithm 1.
207208

3.3 PERSONALIZED FEDERATED LEARNING WITH FEDPER

209 To integrate the aligned latent representations produced by QAP into federated learning, we adopt
210 **FedPer** (Arivazhagan et al., 2020), a widely used personalization strategy. FedPer separates the
211 model parameters into two groups:
212

216 **Algorithm 1** Query Attention Pooling (QAP) for Feature-Dimension Alignment

217 **Input:** Client data $x^{(i)} \in \mathbb{R}^{B \times L \times F_i}$, target dimension d_{qap}
 218 **Output:** Aligned representation $z^{(i)} \in \mathbb{R}^{B \times L \times d_{\text{qap}}}$
 219
 220 **1. Value projection + slot embedding:**
 221 $V = \text{LayerNorm}(W_v(x^{(i)}) + E_i)$
 222 **2. Flatten for attention:**
 223 $x_{\text{flat}} = \text{reshape}(V, [B \cdot L, F_i, d_{\text{qap}}])$
 224 **3. Cross-attention pooling:**
 225 $z = \text{Attention}(Q, x_{\text{flat}}, x_{\text{flat}})$
 226 **4. Statistical fusion:**
 227 $\mu = \text{mean}(x_{\text{flat}})$, $m = \max(x_{\text{flat}})$
 228 $z = \text{MLP}([z; \mu; m])$
 229 **5. Restore temporal structure:**
 230 $z^{(i)} = \text{reshape}(z, [B, L, d_{\text{qap}}])$
 231 **return** $z^{(i)}$

 232 **Notation:** B = batch size, L = sequence length, F_i = number of features for client i , d_{qap} = latent dimension
 233 after QAP alignment, W_v = value projection, E_i = slot embeddings, Q = shared query vector.

 234
 235
 236

237 **(1) Shared backbone**—trained collaboratively across all clients through federated aggregation.
 238
 239 **(2) Personalized heads**—remain local to each client and are never transmitted to the server.

240 In our setting, once QAP maps a client’s raw input with feature dimension F_i into a unified latent
 241 space of size d_{qap} , the shared backbone processes this aligned representation. Importantly, because
 242 QAP already ensures consistent dimensionality across clients, the output can be directly fed into a
 243 wide range of backbone architectures (e.g., transformers, mixers, spiking networks) without requir-
 244 ing any additional preprocessing layers. Each client then applies its own lightweight prediction head
 245 to transform the backbone output back to its original feature dimension F_i .
 246

247 During training, backbone parameters and shared QAP components (queries, value projection, at-
 248 tention layers, fusion networks, normalization, time feature projection, and concatenation fusion)
 249 are uploaded to the server and aggregated. Client-specific components—including slot embeddings
 250 and prediction heads—remain local, ensuring personalized adaptation to each client’s unique fea-
 251 ture space and output requirements. The federated training procedure with QAP-aligned inputs and
 252 FedPer is detailed in Algorithm ??.

254 4 EXPERIMENTS
 255

256
 257 We evaluate FedQAPer on two widely used multivariate time-series benchmarks: **Electricity** (321
 258 features) and **Traffic** (862 features). Both datasets are publicly available through the extensive
 259 repository of Wang et al. (2024b). Importantly, their high-dimensional feature spaces provide a suf-
 260 ficiently large number of variables to construct diverse clients, making them particularly suitable
 261 for our feature-level non-IID experimental design. For our experiments, we set the input sequence
 262 length (look-back window) to 96 time steps, and evaluate forecasting performance under three hori-
 263 zons: 48, 96, and 192 steps. The federated learning setup involves 20 clients, and each client receives
 264 up to 20 features from the total feature space. All clients participate in every global communication
 265 round, ensuring full federation. To ensure reproducibility, we fix the random seed to 42. Each dataset
 266 is split into 80% training, 10% validation, and 10% testing. For feature alignment, we apply QAP
 267 with query count=1 and latent dimension $d_{\text{qap}}=128$. As backbones, we evaluate both ANN-based
 268 models: iTransformer(Liu et al. (2024b)), TimeMixer(Wang et al. (2024a)), DLinear(Zeng et al.
 269 (2022)) and SNN-based models: Spikeformer, SpikeRNN (Lv et al. (2024)). For SNN models, we
 270 apply SNN time step=4.

270 **Algorithm 2** Federated Training with FedPer using QAP

271 **Input:** Global epochs G , local epochs E , learning rate η , clients \mathcal{C}

272 **Output:** Shared parameters θ^s , personalized parameters $\{\theta_i^p\}_{i \in \mathcal{C}}$

273

274 **Initialization:**

275 $\theta^s = \{\theta^{\text{back}}, \theta^{\text{qap-shared}}, \theta^{\text{time}}\}$ ▷ Shared parameters

276 $\theta_i^p = \{\theta_i^{\text{slot}}, \theta_i^{\text{head}}\}$ ▷ Personalized parameters per client

277 **for** round $t = 1$ to G **do**

278 Sample subset $\mathcal{S}_t \subseteq \mathcal{C}$

279 Server broadcasts θ^s to clients $i \in \mathcal{S}_t$

280 **for all** client $i \in \mathcal{S}_t$ **do in parallel**

281 $\theta_i \leftarrow \theta^s \cup \theta_i^p$ ▷ Combine shared and personalized params

282 **for** epoch $e = 1$ to E **do**

283 **for** batch $(x_i, t_i, y_i) \in \mathcal{D}_i$ **do**

284 **1. Forward pass with QAP:**

285 $z_i = \text{QAP}(x_i; \theta^{\text{qap-shared}}, \theta_i^{\text{slot}})$

286 $z_i^{\text{fus}} = z_i + \text{Linear}(t_i; \theta^{\text{time}})$

287 $\hat{y}_i = \text{Head}(\text{Backbone}(z_i^{\text{fus}}; \theta^{\text{back}}); \theta_i^{\text{head}})$

288 **2. Update parameters:**

289 $\theta_i \leftarrow \theta_i - \eta \nabla \mathcal{L}(\hat{y}_i, y_i)$ ▷ Update all params locally

290 **end for**

291 **end for**

292 Send updated θ_i^s (subset of θ_i) to server ▷ Keep θ_i^p local

293 **end for**

294 **Server Aggregation:**

295 $\theta^s \leftarrow \sum_{i \in \mathcal{S}_t} w_i \cdot \theta_i^s$ ▷ FedAvg on shared parameters only

296 **Notation:** \mathcal{S}_t = sampled clients, \mathcal{D}_i = client i 's data, $w_i = |\mathcal{D}_i| / \sum |\mathcal{D}_j|$.

297 **Shared parameters:** Backbone, Time proj, QAP modules (value.proj, queries, attn, fuse, norm).

298 **Personalized parameters:** Client-specific Slot Embeddings, Prediction Head.

301 4.1 MAIN RESULTS

303 As shown in Table 1, FedQAPer consistently outperforms baseline approaches across all backbones
304 and datasets. In particular, the method achieves the best or second-best results in almost every
305 setting, showing both strong accuracy and robustness to different horizons and model architectures.

306 **Metrics.** Since clients possess heterogeneous output feature dimensions, direct aggregation of raw
307 prediction tensors is structurally infeasible. We therefore compute global metrics using dataset-size
308 weighted averaging of locally computed scalar metrics. Specifically, each client i first computes its
309 local MAE averaged over all dimensions, and the server aggregates these as:

311

$$\text{MAE}_{\text{global}} = \sum_{i=1}^N \text{MAE}_i \times \frac{|\mathcal{D}_i|}{\sum_{j=1}^N |\mathcal{D}_j|}$$

312

315 where $|\mathcal{D}_i|$ denotes the size of client i 's local dataset. All metrics are computed on a normalized
316 scale using a StandardScaler fitted on each training split.

317 On the Traffic dataset, FedQAPer combined with iTransformer delivers the lowest error rates,
318 achieving a top performance with an average MSE of 0.378. For the Electricity dataset, the frame-
319 work paired with DLinear achieves an impressive result with an average MSE of 0.182. This demon-
320 strates FedQAPer's ability to find the most effective model backbone for diverse datasets and max-
321 imize its performance. Notably, our framework is proven to be applicable to both ANN and SNN
322 backbones. While ANN models generally exhibit lower error rates and superior performance, the
323 SNN models, although showing slightly higher errors, demonstrate very competitive performance
when considering their potential for optimization on neuromorphic hardware.

Overall, FedQAPer consistently improves prediction accuracy compared to baselines, demonstrating that feature-level alignment through QAP combined with personalized heads provides an effective and versatile solution for federated time-series forecasting.

Table 1: Main results on Electricity and Traffic. Values are **global test** metrics (MSE, MAE). Lower is better.

Model	SNN						ANN						
	iSpikeformer		SpikeRNN		Spikeformer		iTransformer		TimeMixer		DLinear		
Metrics	MSE	MAE	MSE	MAE	MSE	MAE	MSE	MAE	MSE	MAE	MSE	MAE	
Traffic	48	0.371	0.350	0.380	0.340	0.384	0.356	0.358	0.332	0.356	0.333	0.372	0.348
	96	0.401	0.359	0.401	0.354	0.406	0.358	0.387	0.343	0.390	0.348	0.340	0.359
	192	0.416	0.370	0.398	0.352	0.428	0.376	0.392	0.340	0.391	0.338	0.398	0.350
	Avg	0.396	0.360	0.392	0.349	0.409	0.365	0.378	0.337	0.380	0.341	0.391	0.352
Electricity	48	0.229	0.337	0.219	0.331	0.232	0.339	0.216	0.323	0.220	0.325	0.169	0.281
	96	0.244	0.347	0.221	0.331	0.247	0.353	0.215	0.323	0.216	0.322	0.180	0.292
	192	0.231	0.340	0.241	0.341	0.251	0.359	0.229	0.333	0.219	0.327	0.198	0.309
	Avg	0.235	0.342	0.227	0.334	0.244	0.350	0.220	0.326	0.219	0.325	0.182	0.294

4.2 INFERENCE ENERGY ANALYSIS

To validate the energy efficiency of SNN models, we compare the inference energy consumption between the proposed iSpikeformer and the ANN-based iTransformer model. Inference energy is calculated based on operation energy units at the 45nm technology node. MAC (Multiply-Accumulate) operations consume 4.6 pJ, while AC (Accumulate) operations consume 0.9 pJ.

The inference pipeline of iSpikeformer consists of three stages. In the pre-backbone stage, QAP, Slot Embedding, and Time Projection are performed with float operations, consuming MAC energy. In the backbone stage, spike generation by LIF neurons, sparse matmul operations in SSA (Spiking Self-Attention), and MLP blocks are executed with AC operations proportional to the firing rate. In the final head stage, MAC operations are performed again for mean pooling and final prediction. The key energy savings of SNNs stem from the firing rate. While ANNs perform MAC operations for all computations, SNNs perform AC operations only when spikes are fired, achieving energy efficiency through sparsity.

For a fair apple-to-apple comparison, we exclude the pre-backbone and head portions as they are identical for both models, and compare only the backbone energy.

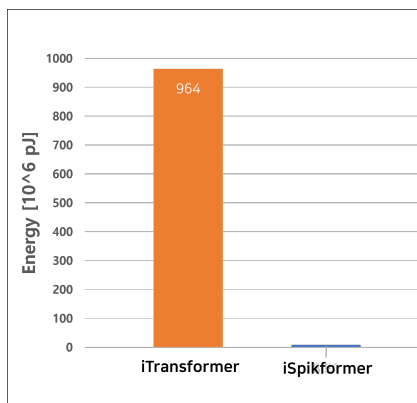


Figure 2: Inference energy comparison between iTransformer and iSpikeformer

The experimental results show that the backbone of iSpikeformer consumes 8.51×10^8 pJ, which is approximately $113 \times$ lower than iTransformer's 9.64×10^{10} pJ. This empirically demonstrates that the spike-based sparse computation of SNNs is advantageous for energy-efficient deployment on edge devices.

378 4.3 ABLATION STUDY
379380 4.3.1 EFFECTIVENESS OF FEDERATED LEARNING
381

382 To isolate the effect of FedPer, we compare federated training, against a *local-only* setting, where
383 each client trains its own model independently for 100 epoch with an early-stopping patience of 20.
384 For local-only results, we report the average test performance across all clients' best models. All
385 results are obtained under a look-back window of 96 and a prediction horizon of 48 time steps.

386 As shown in Table 2, FedPer consistently outperforms local-only training across both datasets. On
387 the **Traffic** dataset, the largest gain is observed with TimeMixer, where FedPer reduces errors by
388 approximately 11% in MSE and 17% in MAE. On the **Electricity** dataset, iTransformer under FedPer
389 reduces MSE by about 33% and MAE by nearly 20% compared to local-only training. For SNN
390 backbones, FedPer also delivers consistent improvements, with error reductions in the range of
391 2–10% compared to local-only training. Overall, these results demonstrate that FedPer not only
392 preserves the strengths of each backbone but also provides clear advantages over isolated local
393 training in feature-level non-IID federated scenarios.

394
395 Table 2: Ablation study: federated vs local-only performance (mean \pm std). Lower is better; best of
396 each pair is highlighted in red bold.

398	Model	Traffic				Electricity				
		MSE		MAE		MSE		MAE		
		Fed	Local	Fed	Local	Fed	Local	Fed	Local	
402	SNN	iSpikeformer	0.379	0.414	0.350	0.396	0.229	0.224	0.337	0.341
		SpikeRNN	0.379	0.443	0.339	0.391	0.221	0.229	0.331	0.337
		Spikeformer	0.384	0.479	0.356	0.414	0.232	0.228	0.339	0.336
405	ANN	iTransformer	0.358	0.692	0.332	0.603	0.216	0.230	0.323	0.334
		TimeMixer	0.356	0.476	0.333	0.433	0.220	0.218	0.325	0.330
		DLinear	0.372	0.612	0.348	0.542	0.169	0.212	0.281	0.320

410 4.3.2 COMMUNICATION EFFICIENCY ANALYSIS
411

412 We analyze the communication efficiency of FedPer compared to conventional federated learning
413 approaches such as FedAvg. Table 3 presents the parameter distribution of our framework.

414 In FedPer, shared parameters (QAP and backbone) account for 578,836 (48.4%), while local param-
415 eters (forecast head) account for 616,160 (51.6%). Notably, the forecast head constitutes over half
416 of the total model parameters.

417 In time series forecasting, the forecast head maps from the hidden dimension to the output predic-
418 tions, and its parameter count scales with $\mathcal{O}(C^2)$, where C denotes the number of features per client.
419 This is because the head must handle client-specific feature dimensions for prediction.

420 In contrast, FedPer only communicates the shared backbone and QAP, whose parameter counts re-
421 main constant regardless of client feature counts, resulting in $\mathcal{O}(1)$ communication cost with respect
422 to C .

423 This architectural choice provides substantial advantages:

- 426 • **Reduced communication overhead:** Only 48.4% of parameters are transmitted during
427 federation, while the largest component (forecast head) remains local.
- 428 • **Scalability:** As feature heterogeneity increases across clients, the communication cost gap
429 between FedAvg and FedPer widens significantly.
- 430 • **Edge device suitability:** The reduced bandwidth requirement enables FedPer to operate
431 effectively on resource-constrained edge devices with limited connectivity.

432

433

Table 3: Parameter distribution across components in our framework.

434

435

436

437

438

439

440

441

These characteristics make FedPer particularly well-suited for federated time series forecasting scenarios with heterogeneous feature counts, limited bandwidth, and predictable communication budgets.

442

443

444

445

446

4.3.3 EFFECTIVENESS OF QUERY-ATTENTION POOLING

447

448

449

450

451

452

453

Also, to **evaluate the effectiveness of QAP**, we compare it against a simple linear projection that only aligns different feature dimensions to a same size. Experiments are conducted on the Traffic dataset. As shown in Table 4, QAP significantly outperforms the linear projection baseline. This demonstrates that QAP not only aligns heterogeneous feature dimensions across clients but also effectively captures important temporal patterns through attention mechanisms. Furthermore, the side channel fusion enables QAP to learn peak and average patterns, leading to improved time series representation learning.

454

455

Table 4: Projection vs QAP comparison across different horizons (mean metrics).

456

457

458

459

460

461

462

463

4.4 CLIENT FEATURE DISTRIBUTION

464

465

To better understand the experimental environment, we visualize the client feature allocation under seed=42. Figure 3 and Figure 4 present two perspectives: the number of features assigned to each client (left) and the pairwise overlap of features across clients (right), for the Electricity and Traffic datasets, respectively. The distributions confirm that our construction enforces completely random feature allocation without any coordination. In both datasets, clients are heterogeneous, each receiving different feature subsets with limited overlap. The Traffic dataset exhibits an extreme case of heterogeneity: several clients are assigned nearly the maximum of 20 features, while others have fewer than five. This stark imbalance occurs because the Traffic dataset has a much larger pool of features (862 total), making it more likely for random sampling to create wide disparities across clients. In contrast, the Electricity dataset, which contains fewer total features (321), produces a comparatively milder but still heterogeneous distribution, with most clients falling between 4 and 12 features and only partial overlap. These observations show that the proposed setup consistently produces heterogeneous clients across datasets, with Traffic serving as a particularly challenging benchmark due to its higher intrinsic feature dimensionality. This confirms that our experimental environment accurately simulates the realistic and difficult non-IID conditions encountered in federated learning.

480

481

482

5 CONCLUSION

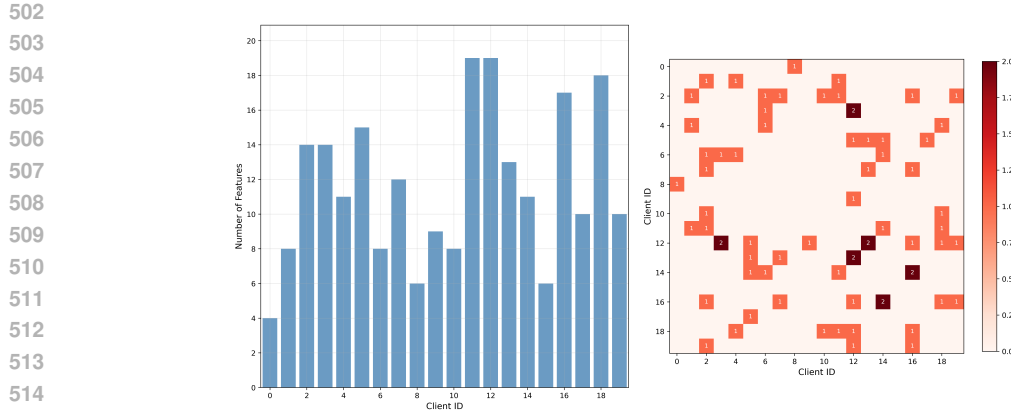
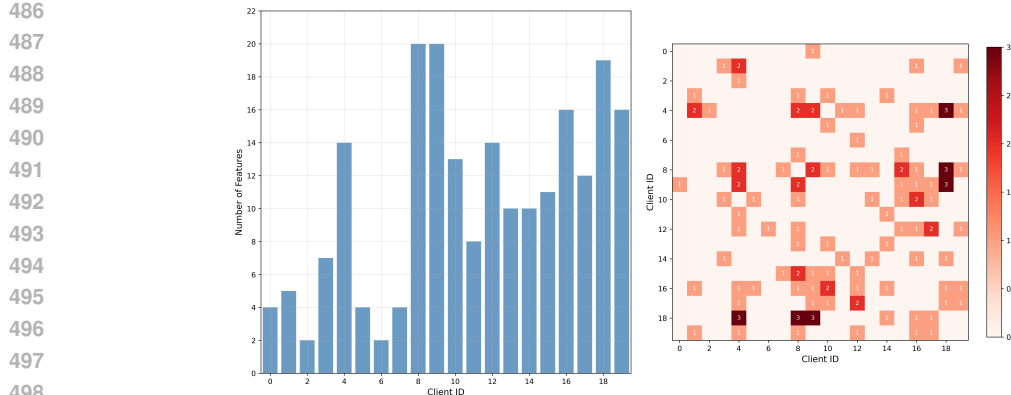
483

484

485

In this work, we presented FedQAPer, a novel federated learning framework that addresses the critical challenge of feature-level heterogeneity in time-series forecasting. Unlike existing FL methods that assume uniform feature spaces across clients, our approach enables effective collabora-

Component	Parameters	Proportion
QAP	167,296	14.0%
iSpikeformer Backbone	412,820	34.5%
Forecast Head	614,880	51.5%
Total	1,194,996	100%



520 tion among clients with diverse feature configurations through the combination of Query Attention
521 Pooling (QAP) and personalized federated learning via FedPer. Our key contributions demonstrate
522 that feature heterogeneity, a common but underexplored challenge in real-world federated deploy-
523 ments, can be effectively managed through dimensional alignment and personalization. The QAP
524 mechanism successfully projects heterogeneous client features into a unified latent space, enabling
525 collaborative training of a shared backbone despite varying input dimensions. Meanwhile, the Fed-
526 Per strategy with personalized heads preserves each client’s ability to capture local patterns specific
527 to their unique feature configurations. Experimental results on the Electricity and Traffic datasets
528 confirm that FedQAPer consistently outperforms both baseline federated approaches and local-only
529 training across multiple backbone architectures, achieving improvements of **up to 33%** in MSE and
530 MAE. The framework’s compatibility with both ANN and SNN models demonstrates its generality
531 and practical applicability. Overall, FedQAPer represents a significant step toward practical feder-
532 ated learning for time-series forecasting in heterogeneous environments, bridging the gap between
533 theoretical FL frameworks and real-world deployments where feature diversity is the norm rather
534 than the exception. For future work, we aim to further enhance FedQAPer’s robustness and flexibil-
535 ity, exploring improved attention variants and more adaptable backbone-head designs to extend its
536 applicability across even more heterogeneous federated scenarios.

537 REFERENCES

538
539 Raed Abdel-Sater and A. Ben Hamza. A federated large language model for long-term time series
forecasting, 2024. URL <https://arxiv.org/abs/2407.20503>.

540 Manoj Ghuhan Arivazhagan, Vinayakumar Aggarwal, Aaditya Singh, and Sunav Choudhary. Federated learning with personalization layers. In *Proceedings of the 23rd International Conference on Artificial Intelligence and Statistics (AISTATS)*, 2020.

541

542

543 Qumrish Arooj. Fedwindt: Federated learning assisted transformer architecture for collaborative and secure wind power forecasting in diverse conditions. *Energy*, 309:133072, 2024. ISSN 0360-5442. doi: <https://doi.org/10.1016/j.energy.2024.133072>. URL <https://www.sciencedirect.com/science/article/pii/S0360544224028470>.

544

545

546

547

548 Sheraz Aslam, Herodotos Herodotou, Syed Muhammad Mohsin, Nadeem Javaid, Nouman Ashraf, and Shahzad Aslam. A survey on deep learning methods for power load and renewable energy forecasting in smart microgrids. *Renewable and Sustainable Energy Reviews*, 144:110992, 2021. ISSN 1364-0321. doi: <https://doi.org/10.1016/j.rser.2021.110992>. URL <https://www.sciencedirect.com/science/article/pii/S1364032121002847>.

549

550

551

552

553 Shuowei Cai and Hao Liu. Hstfl: A heterogeneous federated learning framework for misaligned spatiotemporal forecasting, 2024. URL <https://arxiv.org/abs/2409.18482>.

554

555

556 Luo donghao and wang xue. ModernTCN: A modern pure convolution structure for general time series analysis. In *The Twelfth International Conference on Learning Representations*, 2024. URL <https://openreview.net/forum?id=vpJMJerXHU>.

557

558

559 Mohammad Navid Fekri, Katarina Grolinger, and Syed Mir. Distributed load forecasting using smart meter data: Federated learning with recurrent neural networks. *International Journal of Electrical Power & Energy Systems*, 137:107669, 2022. ISSN 0142-0615. doi: <https://doi.org/10.1016/j.ijepes.2021.107669>. URL <https://www.sciencedirect.com/science/article/pii/S0142061521008991>.

560

561

562

563

564 Shibo Feng, Wanjin Feng, Xingyu Gao, Peilin Zhao, and Zhiqi Shen. Ts-lif: A temporal segment spiking neuron network for time series forecasting, 2025. URL <https://arxiv.org/abs/2503.05108>.

565

566

567

568 Jwaone Gaboitaolelwe, Adamu Murtala Zungeru, Abid Yahya, Caspar K. Lebekwe, Dasari Naga Vinod, and Ayodeji Olalekan Salau. Machine learning based solar photovoltaic power forecasting: A review and comparison. *IEEE Access*, 11:40820–40845, 2023. doi: 10.1109/ACCESS.2023.3270041.

569

570

571

572 Avishek Ghosh, Jichan Chung, Dong Yin, and Kannan Ramchandran. An efficient framework for clustered federated learning, 2021. URL <https://arxiv.org/abs/2006.04088>.

573

574

575 Bang Hu, Changze Lv, Mingjie Li, Yunpeng Liu, Xiaoqing Zheng, Fengzhe Zhang, Wei cao, and Fan Zhang. Spikestag: Spatial-temporal forecasting via gnn-snn collaboration, 2025. URL <https://arxiv.org/abs/2508.02069>.

576

577

578 Sai Praneeth Karimireddy, Satyen Kale, Mehryar Mohri, Sashank J. Reddi, Sebastian U. Stich, and Ananda Theertha Suresh. Scaffold: Stochastic controlled averaging for federated learning, 2021. URL <https://arxiv.org/abs/1910.06378>.

579

580

581 G. Lai, W. C. Chang, Y. Yang, W. Liu, and S. Chien. Electricity consumption dataset, 2018. URL <https://archive.ics.uci.edu/ml/datasets/individual+household+electric+power+consumption>. Accessed: 2025-09-25.

582

583

584

585 Sai Li, Linliang Chen, Yihao Zhang, Zhongkui Zhang, Ao Du, Biao Pan, Zhaohao Wang, Lianggong Wen, and Weisheng Zhao. Quest: A quantized energy-aware snn training framework for multi-state neuromorphic devices, 2025. URL <https://arxiv.org/abs/2504.00679>.

586

587

588 Tian Li, Anit Kumar Sahu, Manzil Zaheer, Maziar Sanjabi, Ameet Talwalkar, and Virginia Smith. Federated optimization in heterogeneous networks, 2020. URL <https://arxiv.org/abs/1812.06127>.

589

590

591

592 Qingxiang Liu, Xu Liu, Chenghao Liu, Qingsong Wen, and Yuxuan Liang. Time-ffm: Towards Im-empowered federated foundation model for time series forecasting, 2024a. URL <https://arxiv.org/abs/2405.14252>.

593

Yixing Liu, Zhen Dong, Bo Liu, Yiqiao Xu, and Zhengtao Ding. Fedforecast: A federated learning framework for short-term probabilistic individual load forecasting in smart grid. *International Journal of Electrical Power & Energy Systems*, 152:109172, 2023. ISSN 0142-0615. doi: <https://doi.org/10.1016/j.ijepes.2023.109172>. URL <https://www.sciencedirect.com/science/article/pii/S0142061523002296>.

Yong Liu, Tengge Hu, Haoran Zhang, Haixu Wu, Shiyu Wang, Lintao Ma, and Mingsheng Long. itransformer: Inverted transformers are effective for time series forecasting, 2024b. URL <https://arxiv.org/abs/2310.06625>.

Changze Lv, Yansen Wang, Dongqi Han, Xiaoqing Zheng, Xuanjing Huang, and Dongsheng Li. Efficient and effective time-series forecasting with spiking neural networks, 2024. URL <https://arxiv.org/abs/2402.01533>.

Mohamed Maher, Osama Fayez Oun, Mahmoud Saeed Mesmeh, and Radwa Elshawi. Fedforecaster: An automated federated learning approach for time-series forecasting. In *Proceedings of the 28th International Conference on Extending Database Technology (EDBT)*, EDBT '25, pp. 867–873, Barcelona, Spain, March 25–28 2025. OpenProceedings.org. ISBN 978-3-89318-099-8. doi: [10.48786/edbt.2025.70](https://doi.org/10.48786/edbt.2025.70).

H. Brendan McMahan, Eider Moore, Daniel Ramage, Seth Hampson, and Blaise Agüera y Arcas. Communication-efficient learning of deep networks from decentralized data, 2023. URL <https://arxiv.org/abs/1602.05629>.

Yuqi Nie, Nam H. Nguyen, Phanwadee Sinthong, and Jayant Kalagnanam. A time series is worth 64 words: Long-term forecasting with transformers, 2023. URL <https://arxiv.org/abs/2211.14730>.

Nicolas Skatchkovsky, Hyeryung Jang, and Osvaldo Simeone. Federated neuromorphic learning of spiking neural networks for low-power edge intelligence, 2019. URL <https://arxiv.org/abs/1910.09594>.

Chu Myaet Thwal, Ye Lin Tun, Kitae Kim, Seong-Bae Park, and Choong Seon Hong. Transformers with attentive federated aggregation for time series stock forecasting. In *2023 International Conference on Information Networking (ICOIN)*, pp. 499–504. IEEE, January 2023. doi: [10.1109/icoin56518.2023.10048928](https://doi.org/10.1109/ICOIN56518.2023.10048928). URL <http://dx.doi.org/10.1109/ICOIN56518.2023.10048928>.

Yeshwanth Venkatesha, Youngeun Kim, Leandros Tassiulas, and Priyadarshini Panda. Federated learning with spiking neural networks. *IEEE Transactions on Signal Processing*, 69:6183–6194, 2021. ISSN 1941-0476. doi: [10.1109/tsp.2021.3121632](https://doi.org/10.1109/tsp.2021.3121632). URL <http://dx.doi.org/10.1109/TSP.2021.3121632>.

Shiyu Wang, Jiawei Li, Xiaoming Shi, Zhou Ye, Baichuan Mo, Wenze Lin, Shengtong Ju, Zhixuan Chu, and Ming Jin. Timemixer++: A general time series pattern machine for universal predictive analysis. *arXiv preprint arXiv:2410.16032*, 2024a.

Yuxuan Wang, Haixu Wu, Jiaxiang Dong, Yong Liu, Mingsheng Long, and Jianmin Wang. Deep time series models: A comprehensive survey and benchmark, 2024b. URL <https://arxiv.org/abs/2407.13278>.

Yuxuan Wang, Haixu Wu, Jiaxiang Dong, Guo Qin, Haoran Zhang, Yong Liu, Yunzhong Qiu, Jianmin Wang, and Mingsheng Long. Timexer: Empowering transformers for time series forecasting with exogenous variables, 2024c. URL <https://arxiv.org/abs/2402.19072>.

Wujie Wen, Xudong Ma, Jinjun Xiong, Wen-mei Hwu, and Yihang Tang. Differentiable spike: A backpropagation-friendly spiking neural network. In *Advances in Neural Information Processing Systems*, volume 36, 2023.

Kan Xie, Zhe Zhang, Bo Li, Jiawen Kang, Dusit Niyato, Shengli Xie, and Yi Wu. Efficient federated learning with spike neural networks for traffic sign recognition. *IEEE Transactions on Vehicular Technology*, 71(9):9980–9992, 2022. doi: [10.1109/TVT.2022.3178808](https://doi.org/10.1109/TVT.2022.3178808).

648 Zhijian Xu, Ailing Zeng, and Qiang Xu. FITS: Modeling time series with \$10k\\$ parameters.
 649 In *The Twelfth International Conference on Learning Representations*, 2024. URL <https://openreview.net/forum?id=bWcnvZ3qMb>.
 650

651 Xicun Yang, JunePyo Jung, Jiliang LU, Keun-Woo Lim, and Leonardo Linguaglossa. MVFL:
 652 Multivariate vertical federated learning for time-series forecasting, 2025. URL <https://openreview.net/forum?id=eP5ICc0584>.
 653

654 Di Yu, Xin Du, Linshan Jiang, Wentao Tong, and Shuguang Deng. Ec-snn: Splitting deep spiking
 655 neural networks for edge devices. In Kate Larson (ed.), *Proceedings of the Thirty-Third Inter-
 656 national Joint Conference on Artificial Intelligence, IJCAI-24*, pp. 5389–5397. International Joint
 657 Conferences on Artificial Intelligence Organization, 8 2024a. doi: 10.24963/ijcai.2024/596. URL
 658 <https://doi.org/10.24963/ijcai.2024/596>. Main Track.
 659

660 Di Yu, Xin Du, Linshan Jiang, Huijing Zhang, and Shuguang Deng. Exploiting label skewness
 661 for spiking neural networks in federated learning, 2025. URL <https://arxiv.org/abs/2412.17305>.
 662

663 Yingchao Yu, Yuping Yan, Jisong Cai, and Yaochu Jin. Heterogeneous federated learning with
 664 convolutional and spiking neural networks, 2024b. URL <https://arxiv.org/abs/2406.09680>.
 665

666 Wei Yuan, Guanhua Ye, Xiangyu Zhao, Quoc Viet Hung Nguyen, Yang Cao, and Hongzhi Yin.
 667 Tackling data heterogeneity in federated time series forecasting, 2024. URL <https://arxiv.org/abs/2411.15716>.
 668

669 Ailing Zeng, Muxi Chen, Lei Zhang, and Qiang Xu. Are transformers effective for time series
 670 forecasting?, 2022. URL <https://arxiv.org/abs/2205.13504>.
 671

672 Yue Zhao, Meng Li, Liangzhen Lai, Naveen Suda, Damon Civin, and Vikas Chandra. Federated
 673 learning with non-iid data. *CoRR*, abs/1806.00582, 2018. URL <http://arxiv.org/abs/1806.00582>.
 674

675 Haoyi Zhou, Shanghang Zhang, Jieqi Peng, Shuai Zhang, Jianxin Li, Hui Xiong, and Wancai Zhang.
 676 Informer: Beyond efficient transformer for long sequence time-series forecasting. In *The Thirty-
 677 Fifth AAAI Conference on Artificial Intelligence, AAAI 2021, Virtual Conference*, volume 35, pp.
 678 11106–11115. AAAI Press, 2021.
 679

680 Tian Zhou, Ziqing Ma, Qingsong Wen, Xue Wang, Liang Sun, and Rong Jin. Fedformer: Fre-
 681 quency enhanced decomposed transformer for long-term series forecasting, 2022. URL <https://arxiv.org/abs/2201.12740>.
 682

683

684 A APPENDIX

685 A.1 DATASET AND METRIC DETAILS

686 **Datasets details** The details of the datasets used in the main experiment are shown in Table 5. The
 687 dataset size in table is organized in (Train, Validation, Test).
 688

689 690 691 692 693 694 695 696 697 698 699 700 701 Table 5: Dataset detailed descriptions

Dataset	Dimension	Frequency	Window length	Horizon length	Dataset size
Traffic	862	Hourly	96	{48, 96, 192}	(14035, 1754, 1754)
Electricity	321	Hourly	96	{48, 96, 192}	(21043, 2630, 2631)

702 **Metric details** We utilize the mean square error (MSE) as loss function and mean absolute error
 703 (MAE) for evaluation. The calculations of these metrics are :

$$704 \text{MSE} = \frac{1}{N} \sum_{i=1}^N (X_i - \hat{X}_i)^2 \quad (1)$$

$$702 \quad 703 \quad 704 \quad \text{MAE} = \frac{1}{N} \sum_{i=1}^N |X_i - \hat{X}_i| \quad 705 \quad 706 \quad 707 \quad 708 \quad 709 \quad 710 \quad 711 \quad 712 \quad 713 \quad 714 \quad 715 \quad 716 \quad 717 \quad 718 \quad 719 \quad 720 \quad 721 \quad 722 \quad 723 \quad 724 \quad 725 \quad 726 \quad 727 \quad 728 \quad 729 \quad 730 \quad 731 \quad 732 \quad 733 \quad 734 \quad 735 \quad 736 \quad 737 \quad 738 \quad 739 \quad 740 \quad 741 \quad 742 \quad 743 \quad 744 \quad 745 \quad 746 \quad 747 \quad 748 \quad 749 \quad 750 \quad 751 \quad 752 \quad 753 \quad 754 \quad 755$$

$$(2)$$

where $X, \hat{X} \in \mathbb{R}^{H \times F}$ denote the ground truth and prediction tensors over horizon H time steps with F features. The metrics are calculated over all $N = H \times F$ prediction elements.

A.2 HYPERPARAMETER SETTING

Backbone Hyperparameter

Table 6 summarizes the backbone architectures and training-related hyperparameters used in our experiments, including a batch size of 128, a learning rate of 1×10^{-3} , and the Adam optimizer.

Table 6: Model architecture hyperparameters. Model-specific parameters are listed in the rightmost column.

Model	Hidden Dim	Layers	Attention Heads	d_{ff}	Kernel Size	Model-specific parameters
iTransformer	512	2 (Encoder)	8	2048	-	Dropout: 0.1, Activation: gelu
TimeMixer	64	2 (PDPM blocks)	-	256	-	Down-sampling: 2, Moving Avg: 25, Top-K: 5
DLinear	-	-	-	-	-	Moving Avg Kernel: 25, Individual: False
SpikeRNN	64	2 (RNN)	-	-	3	Steps: 4, Tau: 2.0, LIF Threshold: 1.0
Spikformer	64	2 (Transformer)	8	256	-	Steps: 4, QK Scale: 0.125, LIF Threshold: 1.0
iSpikformer	128	2	8	512	3	tau: 2.0, Surrogate: ATan, Step: multi-step

QAP Hyperparameter

For the query attention pooling (QAP) module, we set the number of queries to $q = 1$. This choice is motivated by two considerations. First, the sequential nature of time-series data inherently contains continuous temporal dependencies, which can be effectively captured with a single query. Increasing the number of queries provides diminishing returns for modeling temporal continuity in forecasting tasks. Second, reducing the number of queries significantly improves computational efficiency—a critical factor in federated learning where both communication and computation costs scale with the number of participating clients. Hence, $q = 1$ strikes an optimal balance between preserving essential temporal information and minimizing resource overhead in federated settings.

To determine the latent dimension of QAP, we conducted a controlled experiment using the iTransformer backbone, which consistently outperformed other candidates under our baseline setting (batch size = 128, lookback window = 96, horizon = 48, global epochs = 100, local epochs = 1, number of clients = 20, and maximum feature count = 20). We varied d_{qap} across 32, 64, 128, 256 and observed the validation loss. As shown in Figure 5, the loss remained stable for smaller dimensions but increased significantly at 256. The best performance was achieved at $d_{qap} = 128$, which we therefore adopt as our default setting.

A.3 EFFECT OF MAXIMUM FEATURE SIZE

Traffic dataset results under different maximum feature sizes with input length 96, horizon 48, and QAP hidden dimension $d_{qap} = 64$ are shown in Table 7. Bold numbers indicate better performance between $F_{\max} = 20$ and $F_{\max} = 30$. Increasing the number of features per client consistently improves forecasting accuracy across both ANN and SNN backbones, highlighting the benefit of leveraging richer feature contexts in federated learning.

A.4 VISUALIZATION OF QAP TRANSFORMATION

To visualize the effect of QAP, we present an example using the first client from the Electricity dataset, which contains four features. As shown in Figure 6, the raw input time series with four features is transformed by QAP into a 128-dimensional representation ($d_{qap} = 128$). Since visualizing all 128 dimensions is impractical, we show two representative dimensions to illustrate how QAP captures and transforms the temporal patterns from the original features into a unified representation space.

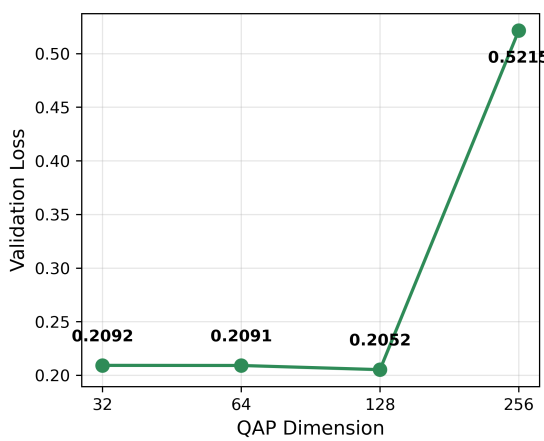


Figure 5: Validation loss across QAP dimensions using the iTransformer backbone. the best result is obtained at $d_{\text{qap}} = 128$.

Table 7: Comparison of forecasting performance with $F_{\text{max}} = 20$ vs $F_{\text{max}} = 30$ on the Traffic dataset.

Model	$F_{\text{max}} = 20$		$F_{\text{max}} = 30$	
	MSE	MAE	MSE	MAE
iTransformer	0.3581	0.3317	0.1502	0.2057
TimeMixer	0.3564	0.3328	0.1701	0.2208
DLinear	0.3719	0.3484	0.1999	0.2390
SpikeRNN	0.3794	0.3392	0.1847	0.2298
Spikformer	0.3845	0.3560	0.1790	0.2449

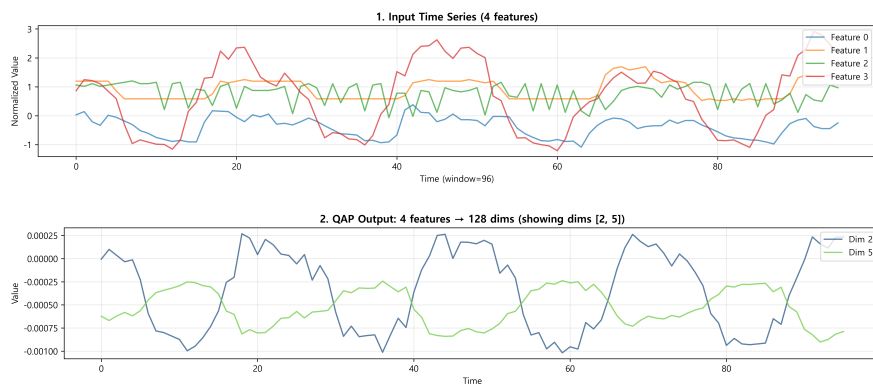


Figure 6: Visualization of QAP transformation on the first client from the Electricity dataset. (Top) Raw input time series with 4 features. (Bottom) Two representative dimensions from the 128-dimensional QAP output.

810 A.5 LIMITATIONS AND FUTURE WORK
811812 While FedQAPer demonstrates promising results under feature-level heterogeneity, several limita-
813 tions remain. First, in the extreme case where a client has only a single feature channel ($F_i = 1$), the
814 attention mechanism of QAP degenerates into a trivial self-attention mapping, reducing its benefit
815 to that of a linear projection. Second, due to the FedPer design that applies personalized heads at
816 the client side, backbone architectures must exclude intrinsic heads to avoid over-parameterization
817 and performance degradation, which restricts the direct use of certain state-of-the-art forecasting
818 backbones.819 As future work, we plan to investigate enhanced QAP variants that can maintain expressiveness
820 even when $F_i = 1$, for instance by incorporating cross-client regularization or slot-level contrastive
821 objectives. In addition, we aim to develop a more flexible backbone–head decoupling mechanism
822 that enables the reuse of head-equipped architectures without redundancy, possibly through selective
823 head freezing or shared head distillation. These directions would further improve the robustness and
824 generality of FedQAPer in diverse practical federated scenarios.825
826
827
828
829
830
831
832
833
834
835
836
837
838
839
840
841
842
843
844
845
846
847
848
849
850
851
852
853
854
855
856
857
858
859
860
861
862
863